This chapter provides a theoretical overview of instrumentation and experimental techniques used to characterize synthesized materials. Nanomaterials and nanocomposites are extensively characterized using X-ray Diffractometer (XRD), Scanning Electron Microscopy (SEM), Transmission Electron Microscopy (TEM), Energy Dispersive Spectroscopy (EDX), Atomic Force Microscopy (AFM), and X-ray Photoelectron Spectroscopy (XPS). Cyclic voltammetry (CV) is used for electrochemical characterization. Additionally, Amperometry i-t curve, Differential Pulse Voltammetry (DPV) and Electrochemical Impedimetric Spectroscopy (EIS) are utilized for electrochemical sensing. Each technique is briefly discussed to provide background information.

2.1 Characterization Techniques

2.1.1 X-ray Diffractometer (XRD)

X-ray Diffraction is a versatile technique offering comprehensive insights into the chemical composition and crystallographic structure of both natural and manufactured materials. Its primary utility lies in identifying and characterizing substances based on their diffraction patterns. In X-ray diffraction, the atoms within a crystal, with their uniform spacing, generate an interference pattern of waves in an incoming X-ray beam, elucidating the material's structure and properties, as depicted in **figure 2.1** [1].

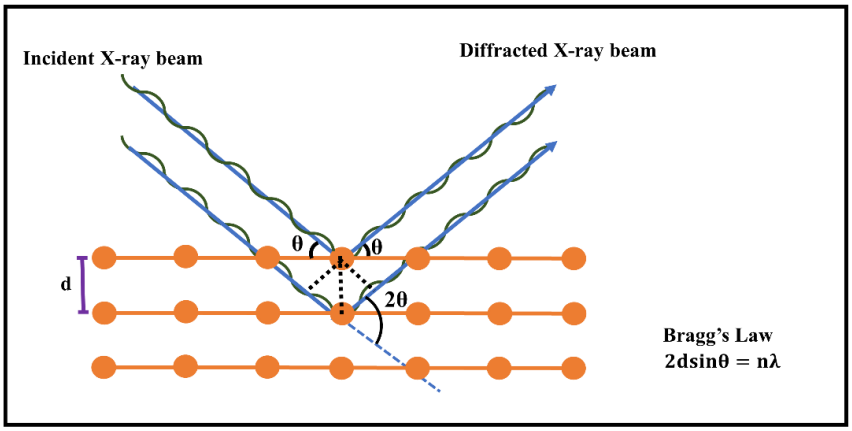

Figure 2.1 Schematic representation of an X-ray beam getting diffracted by a crystallographic material.

X-ray diffraction (XRD) is a technique used to analyze the crystal structure of materials. When monochromatic X-rays interact with a crystal lattice, they are diffracted at specific angles determined by the spacing of atomic planes in the crystal, following Bragg's Law [2].

$$n\lambda = 2dSin\theta$$

This diffraction pattern provides information about the crystal structure, phase composition, and lattice parameters of the material. In powder XRD, the sample is a powder with randomly oriented crystallites. By varying the angle of the X-ray beam, diffraction peaks are observed corresponding to different d-spacing in the material. This technique is sensitive to both the type and relative position of atoms in the material, as well as the length scale over which the crystalline order persists [3,4].

Figure 2.2 Rigaku Miniflex X-ray diffractometer.

The Rigaku MiniFlex X-ray Diffractometer tool used for XRD measurement, using Cu-Kα radiation (λ=1.5405Å) is shown in **figure 2.2**. Calibration is done using silicon powder, and single crystal silicon is used as a standard for obtaining accurate values of 2θ for calculating the quasi-lattice parameter. XRD patterns are collected typically over a range of 10-80° in 2θ, with a step size of 3 °/min.

2.1.2 Scanning Electron Microscopy

An image is formed by a powerful scanning electron microscope (SEM), which utilizes electrons. Imaging of conductive samples at magnifications unachievable by traditional microscopes is enabled. While modern light microscopes achieve up to ~1,000X magnification, magnifications over 30,000X can be reached by typical SEM. Images are in black and white because light is not used in the imaging process by the SEM. Conductive samples are placed on the SEM's sample stage. The sample chamber is vacuumed, and the electron gun is aligned to the correct location by the user. A beam of high-energy electrons is emitted by the electron gun, passing through lenses and apertures before striking the sample. As electrons are continuously shot at the sample by the electron gun at a precise location, secondary electrons bounce off. These secondary electrons are detected by the detector [5]. The signal from the secondary electrons is amplified and displayed on the monitor as a 3D image, being sent there.

Electrons are emitted from a heated electron gun acting as a cathode and accelerated towards the anode, traveling in the same direction as the sample under the influence of a strong electric field. As the electron beam is focused, it passes through the objective lens, which is adjusted by the user to a specific position on the sample.

Upon striking the conductive sample, several interactions occur. Initially, primary electrons penetrate the sample to a depth determined by their energy level. Subsequently, secondary and backscattered electrons are emitted from the sample surface. These emitted electrons are detected by either a secondary electron (SE) or backscattered electron (BS) detector. The detected signals are processed to generate an image of the sample on the screen.

In SE mode, the low-energy secondary electrons are attracted towards the positively biased detector front, and the signal intensity varies with the sample's surface angle, providing detailed topographical images. In contrast, BS mode detects electrons nearly opposite to the beam direction, and the intensity is proportional to the sample's atomic number, yielding less topographical but more compositional information. BS mode is less affected by sample charging, making it suitable for non-conductive samples. The SEM instrument used for characterization is depicted in **figure 2.3.**

Figure 2.3 SEM instrument used for material characterization.

Electrons are emitted from a heated tungsten filament or lanthanum hexaboride (LaB_6) single crystals, accelerated by a voltage typically in the range of 20 V to 30 kV, and directed down an electron optical column consisting of magnetic lenses to produce a focused electron beam that strikes the specimen's surface. The position of the electron beam on the sample is controlled by scanning coils, allowing for scanning over the sample surface. Image formation in the Scanning Electron Microscope (SEM) relies on signals generated from interactions between the electron beam and the sample, specifically inelastic interactions (secondary electrons, SEs) and elastic interactions (backscattered electrons, BSEs).

BSEs provide information from deeper areas of the sample, offering both topographic and compositional details. SEs, on the other hand, originate from surface regions, providing information on topographic contrast and surface texture with good resolution. Most conductive nanomaterials can be directly observed by SEM by loading them on carbon tape. However, non-conductive samples, such as bioorganic nanomaterials, require metal coating (e.g., Gold, Silver, Platinum). In SEM instruments, backscattered and secondary electrons are utilized to construct an image [6,7].

2.1.3 Transmission Electron Microscopy

TEM is the technique where an electron beam is transmitted through an ultra-thin specimen (100nm) which interacts with the specimen as the electron passes through it. The two important features of the TEM are its high lateral spatial resolution and its capability to provide both the image and the diffraction of the sample. This technique is used to obtain the full morphological, crystallographic, atomic structural, microanalytical (chemical composition, bonding),

electronic structure, and coordination number from the samples. **Figure 2.4** depicts the TEM instrument image.

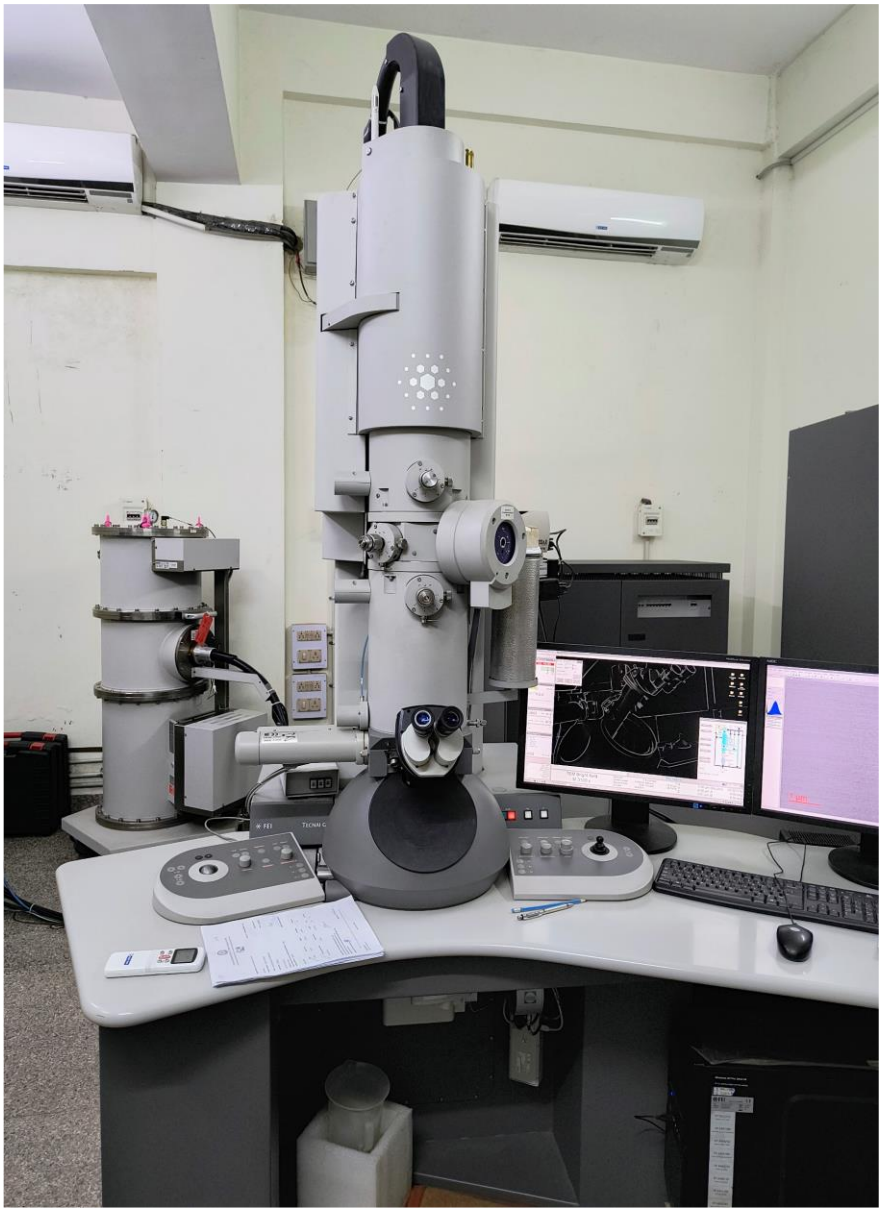

Figure 2.4 TEM instrument used for material characterization.

The TEM works with a high voltage electron beam to create the image, where the electron gun is placed at the top which produces the electron that travels through the vacuum tube. The electromagnetic lens is used to focus the fine beam of electrons that passes through the ultra-thin specimen. The transmitted electrons get hit on the fluorescent screen which is present at

the bottom of the microscope. The image of the specimen with its assorted parts appears on the screen which is based on its density. The obtained image can be directly studied or also photographed [7,8]. TEM analyzes morphological, crystallographic, and compositional information. HR-TEM was produced on the Cu grid using a Tecnai G2 (New Zealand).

2.1.4 Atomic Force Microscope

Atomic force microscopy (AFM) is a powerful tool used to image surfaces at the nanoscale by measuring forces between a sharp probe and a sample. This technique provides high-resolution images and detailed information about surface topography, mechanical properties, and interactions at the atomic level. The AFM equipment utilized in this study for investigating semiconducting materials was provided by NT-MDT Services and Logistics Ltd. (model NTEGRA Prima) in Ireland. The schematic representation of tapping mode in AFM is illustrated in **figure 2.5**. In AFM, a sharp probe, typically a few nanometers in radius, is attached to a cantilever. The cantilever is then scanned across the sample surface in a raster pattern. As the probe interacts with the sample surface, forces such as van der Waals forces, electrostatic forces, and chemical bonding forces cause the cantilever to bend.

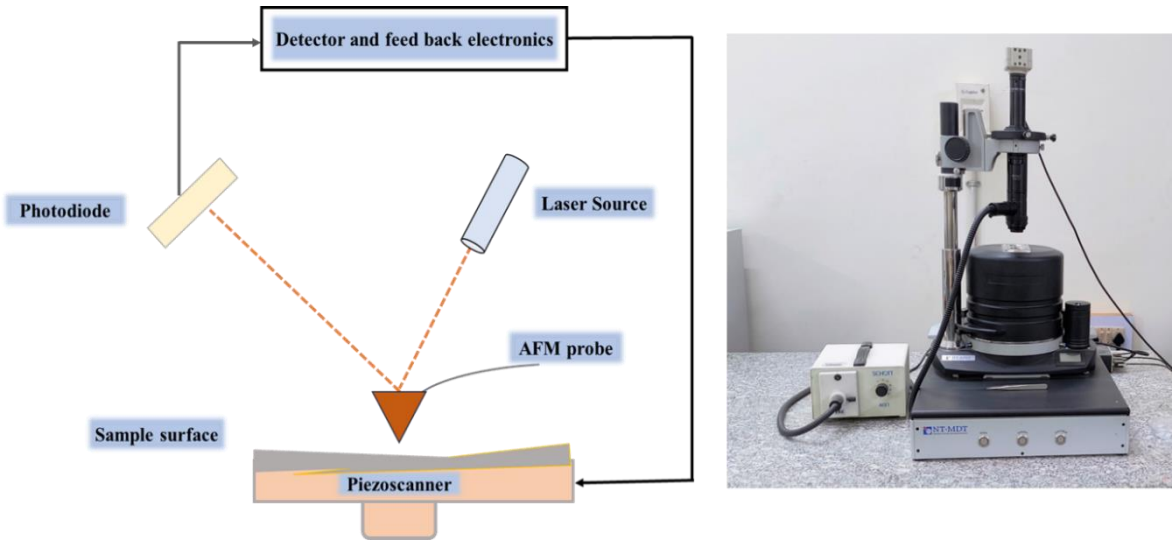

Figure 2.5 The schematic representation of tapping mode in AFM is illustrated along with real image of AFM, NT-MDT Russia.

This bending is detected by a laser beam reflected off the back of the cantilever onto a position-sensitive photodetector. The deflection of the laser beam is used to generate a topographic image of the sample surface with sub-nanometer resolution.

They also have piezoelectric elements, which are electric charges that accumulate in selected solid materials like DNA, biological proteins, crystal, etc., to enable tiny accurate and precise movement during scanning upon an electric command [9].

The Atomic Force Microscope works on the principle measuring intermolecular forces and sees atoms by using probed surfaces of the specimen in nanoscale. Its functioning is enabled by three of its major working principles that include surface sensing, detection, and imaging.

2.1.5 X-ray photoelectron spectroscopy

X-ray photoelectron spectroscopy (XPS) is a surface-sensitive analytical technique. The technique is also recognized as Electron Spectroscopy for Chemical Analysis (ESCA). Quantitative atomic composition and chemistry are determined using X-Ray Photoelectron Spectroscopy. In XPS, a sample is irradiated with a primary beam containing photons and electrons, leading to the emission of secondary electrons from the substrate surface. These secondary electrons are then measured by a spectrometer. In this technique, X-rays are directed at the material surface, and the kinetic energy of the emitted electrons is analyzed. XPS is known for its surface sensitivity and its ability to determine the chemical and oxidation states of elements in a sample. All elements except helium and hydrogen can be identified using XPS. XPS spectra are typically plotted as intensity (count/s) versus binding energy (eV). A wide scan XPS spectrum, known as a survey spectrum, scans from 0 to 1200 eV binding energy. In this study, XPS was used for elemental analysis and to identify the oxidation state of

synthesized nanomaterials and nanocomposites [10,11]. The photoemission measurement principle is shown in **figure 2.6**.

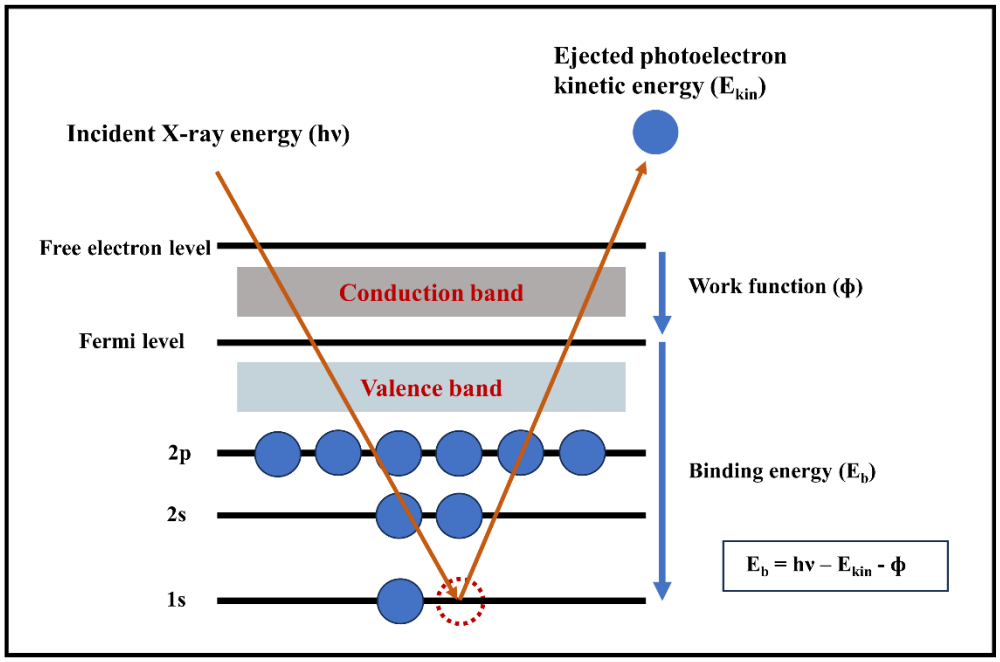

Figure 2.6 Photoemission measurement principle [12].

2.1.6 Fabrication of working electrodes

Working electrode (WE) was fabricated as shown in **figure 2.7.** The mortar and pestle were cleaned thoroughly to remove any residues from previous uses. Measure the required amount of graphite powder using a spatula and place it on the glass plate or weighing paper. To prepare a carbon paste electrode using a mortar and pestle first mix the material thoroughly. Add a few drops of Nujol oil to the graphite powder using a micropipette. Now use the pestle to grind and mix the graphite powder and Nujol oil thoroughly until a homogeneous paste is obtained. The paste should be smooth and easy to manipulate. Filled the carbon paste into the electrode body. The same procedure was followed for fabricating the modified carbon paste electrode by mixing the mediators and nanomaterials with graphite in to the mortar and pestle.

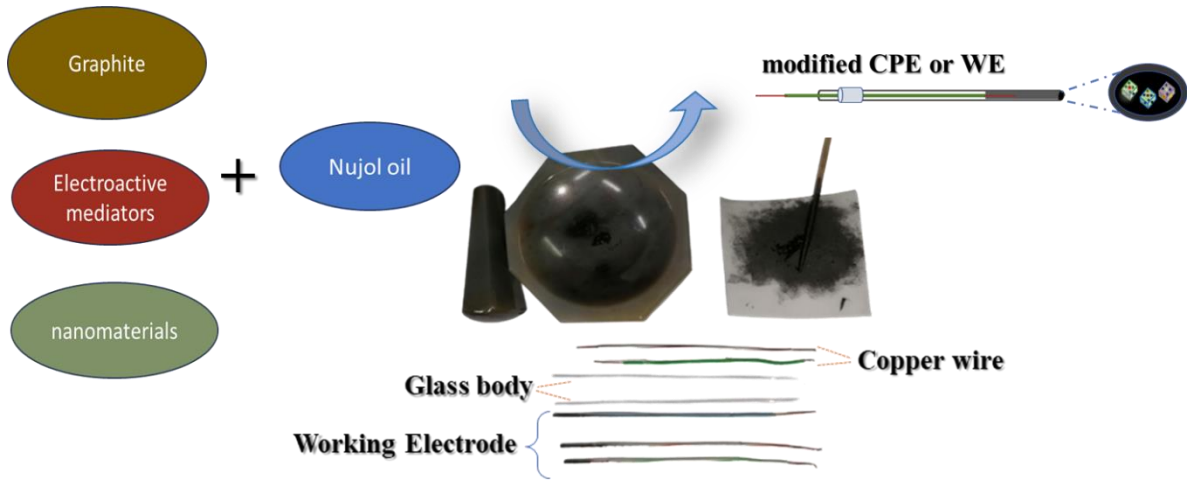

Figure 2.7 Schematic representation for the preparation of working electrode.

2.1.7 Electrochemical Characterization

In this study, electrochemical characterizations of the fabricated electrodes and their responses were conducted using cyclic voltammetry (CV), Differential Pulse Voltammetry (DPV), Amperometry, and Electrochemical Impedance Spectroscopy (EIS) on a CHI 683 B, USA) (as shown in **figure 2.6**). These measurements were performed using a three-electrode assembly to measure current potential as shown in **figure 2.8.**

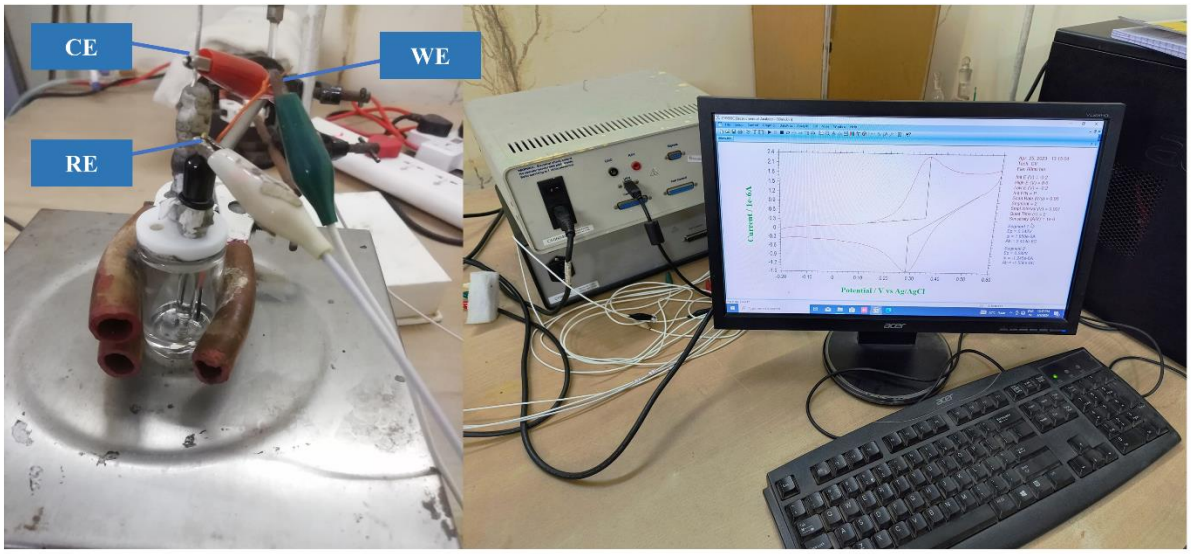

Figure 2.8 Electrochemical workstation and three electrode cell Setup.

The working electrode is sensitive to the analyte's concentration and undergoes the electrochemical redox reaction. The counter electrode completes the electric circuit, while the reference electrode's potential is known with respect to the standard hydrogen electrode (0.00 V) and measures the potential of the working electrode relative to the reference electrode, independent of analyte concentration [13].

Cyclic voltammetry (CV) is a versatile potentiodynamic electroanalytical technique used to investigate the electrochemical properties of electroactive species. The corresponding spectrum of a CV, plotted as current vs. voltage, reflects changes in current corresponding to varying voltage in the solution. CV typically uses microelectrodes in an unstirred solution, limiting the measured current by analyte diffusion at the electrode surface [14]. In a cyclic voltammetry experiment the potential applied between the reference electrode and working electrode increases in a linear fashion with time (scan rate (V/s)). Concomitantly, the current is measured between the working and counter (or auxiliary) electrode resulting in data that is plotted as current (i) vs. potential (E). Reduction and oxidation events are observed and assigned in the resulting plots. Reduction events occur at analyte specific potential voltages where the reaction $M^{+n} + e^- \rightarrow M^{+n-1}$ (M = metal) is energetically favoured (known as reduction potential) and measured by increasing current values. The current will increase as the voltage potential reaches the reduction potential of the analyte, but then falls off as the maximum rate of mass transfer has been reached. The current goes down only to reach equilibrium at some steady value. Oxidation reactions ($M^{+n} \rightarrow M^{+n+1} + e^-$) can also be observed as a decrease in current values at potentials that energetically favor the loss of electron.

The resulting voltammograms are then analyzed and the potential (E_p) and current (I_p) data for both reduction and oxidation events under each setup experimental conditions are noted. This information can be utilized to evaluate the reversibility of coupled reduction and oxidation events. As noted above peak potentials (E_{pa} and E_{pc}) and the peak currents (I_{pc} and I_{pa}) are the fundamental parameters used to characterize a redox couple or event. During a reversible redox process, the oxidized and reduced forms of a compound are in equilibrium at the electrode surface [15,16].

Specifically, the peak current of a reversible reaction is given by Randles-Sevcik equation:

$$\mathrm{I_p} = 2.69 \times 10^5 n^{3/2}\, A\, C\, D^{1/2}\, \nu^{1/2}$$

where, I_p is peak current in amperes, n is the number of electrons involved, A is the area of the electrode in cm^2, D is the diffusion constant (cm^2/s), v is the scan rate (V/s) and C is the bulk concentration (mol/cm^3).

The position of the reduction and/or oxidation events can be used to infer information about the electronic nature of transition metal complexes and the effects on ligands as donors. For example, the $Fe^{3+/2+}$ reduction potential of ferrocene derivatives is very sensitive to the electronic environment provided by the cyclopentadienyl (Cp) ligand set. Electron donating (withdrawing) Cp substituents increase (decrease) the electron density on the iron center and shift the redox potential to negative (positive) values relative to Fc.

In this protocol ferrocene will be used as an example. Experimental conditions such as solvent, electrolyte choice, and the potential range studied (scan window) are largely dictated by analyte solubility and experimental conditions.

Differential pulse voltammetry (DPV) involves superimposing small amplitude, short pulses on a linear ramp. The difference between the currents before and after each pulse is plotted

against potential, minimizing background current and providing a Faradaic current free of most capacitive current. DPV's advantage lies in its low capacitive current, which enhances sensitivity and allows for distinguishing analytes with closely spaced oxidation potentials.

In amperometry, the current (i) is measured as a function of time (t) at a constant applied potential. This technique is commonly used in the electrochemical sensing of biomolecules.

The working principle of amperometry involves applying a constant potential to an electrode, which results in a steady-state current flow due to the oxidation or reduction of electroactive species at the electrode surface. When a biomolecule of interest interacts with the electrode surface, it can either facilitate or hinder the electron transfer process, leading to changes in the current signal that are proportional to the concentration of the biomolecule [17,18].

Electrochemical Impedance Spectroscopy (EIS) utilizes a small amplitude, alternating current (AC) signal to study the impedance characteristics of an electrochemical cell over a range of frequencies [19]. This technique differs from direct current (DC) methods by enabling the study of inductive, capacitive, and diffusion processes within the electrochemical cell [20]. EIS is valuable for studying interfacial properties related to bio-recognition events, making it useful in various biomedical diagnosis and sensing applications.

2.2 References

[1] Martin. Ermrich, Detlef. Opper, PANalytical (Almelo), XRD for the analyst: getting acquainted with the principles, *PANalytical*, 2013.

[2] J. Epp, 4 - X-ray diffraction (XRD) techniques for materials characterization, in: G. Hübschen, I. Altpeter, R. Tschuncky, H.-G. Herrmann (Eds.), Materials Characterization Using Nondestructive Evaluation (NDE) Methods, *Woodhead Publishing*, (2016) 81–124. https://doi.org/https://doi.org/10.1016/b978-0-08-100040-3.00004-3.

[3] C. Hammond, The basics of crystallography and diffraction, Vol. **21**. *Oxford University Press*, *USA*, 2015.

[4] C.F. Holder, R.E. Schaak, Tutorial on Powder X-ray Diffraction for Characterizing Nanoscale Materials, *ACS Nano*, **13** (2019) 7359–7365. https://doi.org/10.1021/acsnano.9b05157.

[5] J.I. Goldstein, D.E. Newbury, J.R. Michael, N.W.M. Ritchie, J.H.J. Scott, D.C. Joy, Scanning Electron Microscopy and X-Ray Microanalysis, *Springer New York*, (2017). https://doi.org/10.1007/978-1-4939-6676-9.

[6] K. Akhtar, S.A. Khan, S.B. Khan, A.M. Asiri, Scanning electron microscopy: Principle and applications in nanomaterials characterization, in: Handbook of Materials Characterization, *Springer International Publishing*, (2018) 113–145. https://doi.org/10.1007/978-3-319-92955-2_4.

[7] B.J. Inkson, Scanning electron microscopy (SEM) and transmission electron microscopy (TEM) for materials characterization, Materials Characterization Using Nondestructive Evaluation (NDE) Methods, *Woodhead publishing*, (2016) 17–43. https://doi.org/10.1016/b978-0-08-100040-3.00002-x.

[8] T. Walther, Transmission Electron Microscopy of Nanostructures, Microscopy Methods in Nanomaterials Characterization, *Elsevier*, (2017) 105–134. https://doi.org/10.1016/B978-0-323-46141-2.00004-3.

[9] R. Bellotti, G.B. Picotto, L. Ribotta, AFM Measurements and Tip Characterization of Nanoparticles with Different Shapes, *Nanomanufacturing Metrol.*, **5** (2022) 127–138. https://doi.org/10.1007/s41871-022-00125-x.

[10] D.N.G. Krishna, J. Philip, Review on surface-characterization applications of X-ray photoelectron spectroscopy (XPS): Recent developments and challenges, *Appl. Surf. Sci. Adv.*, **12** (2022). https://doi.org/10.1016/j.apsadv.2022.100332.

[11] M.A. Isaacs, J. Davies-Jones, P.R. Davies, S. Guan, R. Lee, D.J. Morgan, R. Palgrave, Advanced XPS characterization: XPS-based multi-technique analyses for comprehensive understanding of functional materials, *Mater*. *Chem*. *Front*., **5** (2021) 7931–7963. https://doi.org/10.1039/d1qm00969a.

[12] E. Mazzotta, S. Rella, A. Turco, C. Malitesta, XPS in development of chemical sensors, *RSC Adv*., **5** (2015) 83164–83186. https://doi.org/10.1039/c5ra14139g.

[13] E. Bakker, M. Telting-Diaz, Electrochemical sensors, *Anal*. *Chem*., **74** (2002) 2781–2800. https://doi.org/10.1021/ac0202278.

[14] O. Gilbert, B.E. Kumara Swamy, U. Chandra, B.S. Sherigara, Simultaneous detection of dopamine and ascorbic acid using polyglycine modified carbon paste electrode: A cyclic voltammetric study, *J*. *Electroanal*. *Chem*., **636** (2009) 80–85. https://doi.org/10.1016/j.jelechem.2009.09.016.

[15] F. Harnisch, S. Freguia, A basic tutorial on cyclic voltammetry for the investigation of electroactive microbial biofilms, *Chem*. *Asian J*., **7** (2012) 466–475. https://doi.org/10.1002/asia.201100740.

[16] F. Marken, A. Neudeck, A.M. Bond, Cyclic voltammetry, in: Electroanalytical Methods: Guide to Experiments and Applications, *Springer Berlin Heidelberg*, (2010) 57–106. https://doi.org/10.1007/978-3-642-02915-8_4.

[17] B. Kashyap, R. Kumar, A novel multi-set differential pulse voltammetry technique for improving precision in electrochemical sensing, *Biosens*. *Bioelectron*., **216** (2022). https://doi.org/10.1016/j.bios.2022.114628.

[18] S. Tajik, Z. Dourandish, P.M. Jahani, I. Sheikhshoaie, H. Beitollahi, M. Shahedi Asl, H.W. Jang, M. Shokouhimehr, Recent developments in voltammetric and amperometric sensors for cysteine detection, *RSC Adv*., **11** (2021) 5411–5425. https://doi.org/10.1039/d0ra07614g.

[19] F. Lisdat, D. Schäfer, The use of electrochemical impedance spectroscopy for biosensing, *Anal*. *Bioanal*. *Chem*., **391** (2008) 1555–1567. https://doi.org/10.1007/s00216-008-1970-7.

[20] A.C. Lazanas, M.I. Prodromidis, Electrochemical Impedance Spectroscopy-A Tutorial, *ACS Meas*. *Sci*. *Au*, **3** (2023) 162–193. https://doi.org/10.1021/acsmeasuresciau.2c00070.